CMS Physics Analysis Summary

Contact: cms-pag-conveners-top@cern.ch 2014/10/21

Measurements of the differential cross section of single top-quark production in the t channel in proton-proton collisions at $\sqrt{s} = 8\,\text{TeV}$

The CMS Collaboration

Abstract

Measurements of differential single top quark t channel production cross sections in proton-proton collisions are presented. The differential cross sections are measured as functions of the transverse momentum and the absolute value of the rapidity of the top quark. The analysis is performed in the leptonic decay channels of the top quark, with either a muon or an electron in the final state, using data collected with the CMS experiment at the LHC at a centre-of-mass energy of 8 TeV and corresponding to an integrated luminosity of 19.7 fb^{-1}. Artificial neural networks are used to discriminate the signal process from the various background contributions. The results are found to agree with predictions from Monte Carlo generators.

1 Introduction

The electroweak production of single top quarks has been discovered and established by measurements at the Tevatron at Fermilab [1, 2] and the CERN LHC [3, 4]. A variety of theory calculations and Monte Carlo (MC) generator programs exists that calculate single-top quark production, within the standard model and beyond, using different approaches and approximations. Differential measurements of production cross sections are particularly well suited to assess the accuracy of the predictions. Different MC generators use different implementations for the modeling of the b quarks in the initial state of single top-quark production in the t channel. While in the so-called "five-flavor" scheme the b quark is treated in the same way as the other four lighter quarks, namely it is included in the parton distribution function of the proton, in the "four-flavor" scheme the b quarks are treated independently. The different approaches have both advantages and disadvantages regarding the prediction of the inclusive cross section and description of the kinematics of the involved particles [5].

In the analysis described in this note, the differential cross section of single top quark production in the t channel is measured as a function of the transverse momentum and the absolute rapidity of the top quark. The measurement is performed using data of proton-proton collisions recorded at the CMS experiment at the LHC at a centre-of-mass energy of 8 TeV and corresponding to an integrated luminosity of 19.7 fb^{-1}. The leptonic decay channels of the top quarks with either a muon or an electron in the final state are analysed. A similar analysis at a centre-of-mass energy of 7 TeV has been recently reported by the ATLAS collaboration [3].

2 Data and simulation

The full 8 TeV dataset recorded by the CMS experiment is used for the analysis documented in this note. After correcting for periods of time in which the CMS detector was not fully operational, this dataset corresponds to an integrated luminosity of 19.7 fb^{-1}. For comparison of the data with theory predictions and for the determination of selection efficiencies, samples of simulated signal and background events are used. The signal process of single top-quark production in the t channel as well as the other single top-quark production channels are simulated using the Monte Carlo event generator POWHEG [6–9] interfaced to PYTHIA version 6 [10] for the simulation of hadronization and parton shower. The background contribution from the top quark anti-quark pair production ($\text{t}\bar{\text{t}}$) is simulated using MADGRAPH [11], also interfaced to PYTHIA. For all samples containing events with top quarks a generated top-quark mass of 172.5 GeV is used. The same combination of MADGRAPH and PYTHIA is used to generate the background from the production of W or Z bosons in association with jets (W+jets and Z+jets). The diboson processes (WW, WZ, and ZZ) are simulated using PYTHIA. All samples of simulated events are overlaid with additional collision interactions (pileup) as measured in the data.

The cross section, calculated at approximate next-to-next-to-leading order (NNLO) [12], is 56.4 pb (30.7 pb) for top (anti-)quark production via the t channel, 3.79 pb (1.79 pb) for top (anti-)quark production via the s channel, and 22.2 pb for inclusive production in the tW channel. The predicted $\text{t}\bar{\text{t}}$ production cross section is $252.9^{+6.4}_{-8.6}\,(\text{scale}) \pm 11.7\,(\text{PDF} + \alpha_S)$ pb as calculated with the TOP++2.0 program to next-to-next-to-leading order in perturbative QCD, including soft-gluon resummation to next-to-next-to-leading-log order (see [13] and references therein). NNLO predictions for W boson production with two, three, and four or more jets are 2159.20 pb, 640.40 pb, and 264.00 pb, calculated using FEWZ[14]. The production of W bosons with zero or one jets has been found to be negligible for this analysis. With the same method

the cross section at NNLO for Z+ jets production is calculated to be 3503.71 pb. The cross sections at NLO for the production of two vector bosons are 54.83 pb (WW), 33.21 pb (WZ), and 8.05 pb (ZZ), calculated using MCFM [15].

Although the cross section for QCD multijet production is very large, the probability for such an event to mimic the final state of the signal process is very small. As a result it becomes impractical to simulate enough events for this process to have a reliable quality of the simulation. The QCD multijet processes are modeled using data from a sideband region enriched in such events. This data-driven modeling of the QCD multijet background component is described in the next section.

3 Event selection

Events are selected that contain exactly one isolated electron or muon, one b-tagged jet, one light-quark jet and significant amounts of missing transverse energy or transverse W boson mass, depending on the decay channel. Events containing a tau lepton decaying to a muon or an electron are also accepted if the resulting electron or muon satisfies the applied requirements.

The first stage of event selection are the trigger paths, which require the presence of an isolated electron or muon. For the reconstruction of selected events the particle-flow (PF) [16, 17] algorithm is used, which reconstructs and identifies each single particle combining information from all detector components.

In the muon+jets channel the presence of exactly one isolated muon candidate with transverse momentum p_{T} >26 GeV is required, that is detected within the trigger acceptance range ($|\eta| < 2.1$) and fulfills a set of additional muon identification criteria, referred to as "tight muon ID" [18]. The pseudo rapidity η is defined as $\eta = -\ln[\tan(\theta/2)]$. The "particle flow relative isolation" ($\mathrm{I_{rel}}$) is defined as

$$\mathrm{I_{rel}} = \frac{\mathrm{I^{ch}} + max((\mathrm{I}^{\gamma} + \mathrm{I^{nh}} - \mathrm{I^{PU}}), 0)}{p_{\mathrm{T}}}\,, \tag{1}$$

where $\mathrm{I^{ch}}$, I^{γ}, and $\mathrm{I^{nh}}$ are the sums of the transverse energies deposited by stable charged hadrons, photons, and neutral hadrons in a cone of size $\Delta R = \sqrt{(\Delta\eta)^2 + (\Delta\phi)^2} = 0.4$ around the muon direction. The sum of the transverse momenta of all tracks associated to non-leading vertices is used to estimate the contribution of neutral particles from pileup events, $\mathrm{I^{PU}} \equiv 0.5 \times \sum p_{\mathrm{T}}^{\mathrm{PU}}$. A multiplicative factor 0.5 is applied that takes into account the ratio of neutral particles to charged particles as expected from iso-spin invariance. For the muon to be considered isolated, $\mathrm{I_{rel}}$ should be less than 0.12.

Similarly, in the electron+jets channel, the presence of an isolated electron candidate with $E_{\mathrm{T}} > 30$ GeV and $|\eta| < 2.5$ is required. Electron candidates are identified using a set of variables describing the quality of the track, the shape of the energy deposits in the electromagnetic calorimeter, and the compatibility of the information from tracker and electromagnetic calorimeter, combined into one multivariate discriminant [19]. For the calculation of the relative isolation in the electron channel the effective area corrections are used:

$$\mathrm{I_{rel}} = \frac{\mathrm{I^{ch}} + max((\mathrm{I}^{\gamma} + \mathrm{I^{nh}} - \rho \times A), 0)}{p_{\mathrm{T}}}\,, \tag{2}$$

where ρ is the average energy of the particles not used to reconstruct jets and A is the area of the jet in the $\eta - \phi$ plane. The values of ρ are calculated using the jets built with the k_T algorithm [20] with a distance parameter of 0.6. An isolation cone of $\Delta R = 0.3$ is optimum for the reconstruction of electrons. Electron candidates are considered isolated if $I_{rel} < 0.1$.

To suppress background contributions from events containing more than one electron or muon, events with additional more loosely defined electron or muon candidates are rejected. The loose muon or electron candidates are defined by a minimum transverse momentum of $p_T >$ 10 GeV (muon) or a minimum transverse energy of $E_T > 20$ GeV (electron), $|\eta| < 2.5$, and a relaxed isolation requirement of $I_{rel} < 0.2$. Also the criteria on the muon or electron ID are relaxed.

Jets are reconstructed from all PF particle candidates, using the anti-k_T algorithm [21] with a distance parameter of 0.5. The jet energy is scaled by a factor that describes the detector response depending on the transverse energy and the pseudo rapidity of the jet [22]. Jets with transverse momenta $p_T > 40$ GeV and $|\eta| < 4.5$ are selected. The final-state event topology of single top-quark production in the t channel features a spectator b quark, coming from the initial gluon splitting. As this second b quark has a soft transverse momentum distribution, in most of the events the corresponding b jet fails the transverse momentum requirement and is therefore not selected. Another special feature of the t channel production of single top quarks is that the light quark in the final state is more likely to be found in the forward region. This feature can be used to suppress the major background contributions coming from $t\bar{t}$ and W+jets production. For that reason an extended pseudo rapidity requirement is applied in the jet selection.

The PF jets must have more than one constituent, neutral hadronic and neutral electro-magnetic energy fractions smaller than 99%, and if the jet is in the central region ($|\eta| < 2.4$) it must have a charged electro-magnetic energy fraction below 99% and a non-zero charged hadronic energy fraction and charged particle multiplicity. To distinguish between jets consistent with originating from a b-quark hadronization and jets coming from light quarks or gluons, the b-tagging discriminator of the "Combined Secondary Vertex Tagger" (CSV) [23] is used at its tight working point with a mistag rate on the order of 0.1% and a corresponding tagging efficiency of about 40% to 60%, depending on the actual jet p_T and jet η.

The number of required jets and b tags defines the signal region as well as different control regions enriched in certain background processes, which are used to validate the simulation of the background processes with data. The signal region is defined by requiring exactly two jets, one of which has to be tagged as b jet ("2j1t"). Only these events are used for the final differential cross section measurements. Inverting the b tag requirement leads to the control region enriched in W+jets events ("2j0t"), while the control region for $t\bar{t}$ is defined by three jets, of which exactly two have to be identified as b jets ("3j2t").

In order to reject SM-background events which do not contain neutrinos in the final state, two related quantities are exploited in the two channels. In the electron channel the missing transverse energy is required to be larger than $E_T^{miss} = |\vec{\not{E}}_T| > 45\,\text{GeV}$. The $\vec{\not{E}}_T$ is defined as the negative vectorial sum of transverse momenta of all identified particle flow particles. In the muon channel events without neutrinos are rejected by the requirement $m_{T,W} > 50$ GeV, where $m_{T,W}$ is the transverse mass of the reconstructed W boson candidate, defined as

$$m_{T,W} = \sqrt{\left(p_{T,l} + |\vec{\not{E}}_T|\right)^2 - \left(p_{x,l} + \vec{\not{E}}_{Tx}\right)^2 - \left(p_{y,l} + \vec{\not{E}}_{Ty}\right)^2}, \quad (3)$$

where $p_{\mathrm{T},l}$ is the transverse momentum of the charged lepton, $p_{x,l}$ and $p_{y,l}$ are the x and y components of the charged lepton momentum and $\vec{\not{E}}_{\mathrm{T}x}$ and $\vec{\not{E}}_{\mathrm{T}y}$ are the x and y components of $\vec{\not{E}}_{\mathrm{T}}$.

As mentioned before the distributions for QCD multijet processes are modeled directly from data. For that reason one of the described selection requirements is altered to define sidebands of the 2j1t and 3j2t regions that are enriched in QCD events. Instead of requiring $\mathrm{I}_{\mathrm{rel}} < 0.12$ for the muon and $\mathrm{I}_{\mathrm{rel}} < 0.1$ for the electron candidates, for the definition of the QCD enriched sideband regions the isolation of the lepton has to be between 0.3 and 0.5.

4 Neural network classification and background estimation

After the application of the event selection criteria described in the previous section, the amount of remaining background events is still dominant. It is however possible to further separate the signal processes from the background contributions by simultaneously exploiting the differences in various kinematic variables using multivariate analysis (MVA) methods. In the analysis described in this note the artificial neural network (NN) implemented in the NeuroBayes package [24, 25] is utilized. This MVA tool is a feed-forward NN with one input layer, one hidden layer, and one output layer. In addition to global event variables the neural net uses kinematic variables of the reconstructed top quark. For that purpose a reconstruction of the full event under the assumption of a single top-quark event is applied. The following section gives a brief overview over the applied reconstruction algorithm followed by a description of the used input variables and a description on how the NN output is used in order to reduce the amount of background contributions and to estimate the remaining background fraction.

4.1 Top-quark reconstruction

In this analysis the leptonic decay of the W boson is considered. Thus the reconstruction of the top quark starts with the reconstruction of the four-vector of the W boson from the detected electron or muon and the missing transverse energy vector in the event. The transverse components of the neutrino momentum are taken from the missing transverse energy. The z component of the neutrino momentum is determined from a quadratic equation using the W boson mass as a constraint. In about two thirds of all events this approach results in two real solutions for the missing z component and the solution with the smallest value of $|P_{z,\nu}|$ is chosen. This choice is justified by studies on simulated signal events. In about one third of the events the reconstructed transverse mass of the W boson is larger than the W boson pole mass used as constraint, which leads to complex solutions of the quadratic equation. The imaginary part of the solution is eliminated by modifying the components of the missing transverse energy (and thus the transverse neutrino momentum components) such that $m_{\mathrm{T,W}} = m_{\mathrm{W}}$ while they still satisfy the initial assumption [26].

For the signal region (2j1t) the assignment of the selected jets to the final state quarks is straight forward: the tagged jet is assigned to the b quark from the top-quark decay and the other jet is assigned to the light quark in the final state.

In the control region with two jets and no b tag (2j0t) which is used to check the modeling of the W+jets process, the jet-quark assignment is done based on the pseudo rapidity of the two jets. The most forward jet is assigned to the light quark in the final state and the other jet is assigned to the b quark from the top-quark decay.

In the control region with three jets and two b tags (3j2t) which is used to check the model of

the $t\bar{t}$ process, the jet-quark assignment is done in the following way: The jet with the lowest b tagging discriminator value is assigned to the light quark and for the remaining jets the invariant masses of the reconstructed top quarks using each jet candidate are calculated and the jet yielding the mass value that is closest to the true top-quark mass of 172.5 GeV is assigned to the b quark from the top-quark decay. The remaining jet is assigned to the second b quark in the event, assuming the single top-quark event topology in the t channel, where an additional b jet is assumed to stem from the initial gluon splitting into a $b\bar{b}$ pair.

4.2 Input variables

The training is done in the 2j1t region, separately for the muon and the electron channels. The neural net is trained with t-channel events as signal and $t\bar{t}$, W+jets, and Z+jets events as background with equal numbers of events for the signal and the combined background. The three background processes are weighted according to their cross sections and combined into one background sample. Only those variables are used that are well modeled by the Monte Carlo simulation – checked in the W+jets and $t\bar{t}$ enriched control regions – and that add a significant amount of discrimination power with respect to the training without using this variable. The same discriminator obtained from training in the 2j1t region is then applied to all three categories (2j0t, 2j1t, 3j2t).

The variables used in the trainings are briefly described below. The two most discriminating variables are the pseudo rapidity of the light quark jet, η_{lq}, and the invariant mass of the reconstructed top-quark candidate, $m_{\ell,\nu,b}$. Further discriminating variables are the invariant mass of the dijet-system of the two leading jets, $m_{jet1jet2}$, and with less separation power the invariant masses of the individual two leading jets, m_{jet1} and m_{jet2}. The transverse mass of the reconstructed W boson, $m_{\mathrm{T,W}}$, the charge of the selected lepton, Q_ℓ, and the pseudo rapidity of the reconstructed W boson, η_W, have also a large discrimination power in both channels. In addition to its pseudo rapidity the invariant mass, m_{lq}, and the transverse momentum, $p_{\mathrm{T},lq}$, of the jet assigned to the light quark in the final state contribute to the discrimination power. Some discrimination power comes from the differences in ϕ between the lepton and the light quark jet, $\Delta\phi(\ell, lq)$, and between the second leading jet and missing transverse energy, $\Delta\phi(jet2, \vec{\not{E}}_{\mathrm{T}})$, as well as from the angular difference between the leading jet and $\vec{\not{E}}_{\mathrm{T}}$, $\Delta R(jet1, \vec{\not{E}}_{\mathrm{T}})$, and the missing transverse energy, $E_{\mathrm{T}}^{\mathrm{miss}}$, itself. The common set of variables used in both channels is completed by the event shape variables C and D. The C and D parameters are derived from the eigenvalues λ_i of the linearized momentum tensor ($C = 3 \times (\lambda_1\lambda_2 + \lambda_2\lambda_3 + \lambda_3\lambda_1)$ and $D = 27(\lambda_1\lambda_2\lambda_3)$) and are used to measure the 3-jet and 4-jet structure of an event, respectively.

In addition to this common set of variables, for the training in the muon channel the invariant mass of the jet assigned to the b quark from the top-quark decay, $m_{b_{top}}$, and $\Delta\phi(jet1, \vec{\not{E}}_{\mathrm{T}})$ are used as input variables. For the training in the electron channel the ϕ difference between the second leading jet and the charged lepton, $\Delta\phi(jet2, \ell)$, and the event shape variable aplanarity are used. The latter is calculated from the third largest eigenvalue of the quadratic momentum tensor ($A = \frac{3}{2}\lambda_3$) and measures the transverse momentum component out of the event plane. Table 1 summarizes the used input variables along with their ranks in the two channels, based on their relevance.

4.3 Background rejection and estimation

In the NN output distribution the signal events (S) accumulate at the right half of the distribution while the background events (B) get shuffled to the left part of the distribution. This distinct feature can be used to enrich the selected sample in signal events by cutting on the

Table 1: List of input variables used in the neural network training, ranked by relevance in the two channels.

	rank in channel			rank in channel	
variable	μ+jets	e+jets	variable	μ+jets	e+jets
η_{lq}	1	1	C	11	12
$m_{\ell,\nu,b}$	2	2	$p_{T,lq}$	12	9
$m_{\mathrm{jet1,jet2}}$	3	3	D	13	17
$m_{\mathrm{T,W}}$	4	4	m_{jet1}	14	5
Q_ℓ	5	6	$E_{\mathrm{T}}^{\mathrm{miss}}$	15	14
m_{lq}	6	13	$\Delta\phi[jet2, \vec{\not{E}}_{\mathrm{T}}]$	16	16
η_{W}	7	7	m_{jet2}	17	8
$\Delta\phi[\ell, lq]$	8	11	$\Delta R[jet1, \vec{\not{E}}_{\mathrm{T}}]$	18	15
$m_{b_{top}}$	9	–	$\Delta\phi[jet2, \ell]$	–	10
$\Delta\phi[jet1, \vec{\not{E}}_{\mathrm{T}}]$	10	–	$Aplanarity$	–	18

NN output value thus rejecting a large fraction of the background contributions while keeping a high signal efficiency. The different shapes of signal and background are also used to determine the contributions from the different processes to the selected sample. The optimal cut value is then found by scanning the NN discriminator output distribution from -1 to 1 and comparing the resulting figure of merit $S/\sqrt{S+B}$ for the different cut values. In the muon (electron) channel a value of $Discriminator > 0.3(0.4)$ was found to yield the best figure of merit. The distributions of the top-quark transverse momentum and rapidity are however very stable with respect to the chosen cut value. This has been verified in studies on simulated signal events.

The estimation of the remaining background contributions is done in three steps. In a first step, the amount of QCD multijet events is estimated directly from the data. In the second step the NN output distributions are used to estimate the contribution from other background categories. In the final step these estimations are then extrapolated from the full signal region to the phase space with the cut on the NN output applied.

The estimation of the contribution from QCD multijet background events makes use of the discrimination power of the distribution of the missing transverse energy in the electron channel and the transverse mass of the W boson in the muon channel. Both variables are used in the pre-selection in order to reduce the amount of QCD events. A binned maximum likelihood fit is performed to the $m_{\mathrm{T,W}}$ ($E_{\mathrm{T}}^{\mathrm{miss}}$) distribution in the low-$m_{\mathrm{T,W}}$ (low-$E_{\mathrm{T}}^{\mathrm{miss}}$) sideband region defined by $m_{\mathrm{T,W}} < 50\,\mathrm{GeV}$ ($E_{\mathrm{T}}^{\mathrm{miss}} < 45\,\mathrm{GeV}$) and the result is extrapolated into the signal region, defined by $m_{\mathrm{T,W}} > 50\,\mathrm{GeV}$ in the muon channel and $E_{\mathrm{T}}^{\mathrm{miss}} > 45\,\mathrm{GeV}$ in the electron channel. The templates for all non-QCD processes are derived from the Monte Carlo simulation and are split into one template including all processes with real W bosons and a second template with Z+jets events. As described in Section 3, the fit templates for QCD multijet events are obtained directly from the data in QCD enriched sidebands.

The amount of signal events and the contributions from the remaining background processes are determined with a binned likelihood fit to the NN output distributions, separately for the electron and muon channel (the amount of QCD events is kept fixed to the results obtained from the dedicated QCD-fit). In each channel the output distributions of the NN trained in the signal region (2j1t) and applied to signal region and the $\mathrm{t\bar{t}}$ control region (3j2t) are fit simultaneously in order to gain more power on constraining the fraction of $\mathrm{t\bar{t}}$ events. Background processes are constrained in the fit using Gaussian prior uncertainties. The prior uncertainty

on $\mathrm{t\bar{t}}$ is 20%, prior uncertainties on other backgrounds are 30%. Figure 1 shows the NN output distributions in the two channels for the signal region and the $\mathrm{t\bar{t}}$ control region with the fit templates normalized to the results of the fit. The small visible differences between data and simulation are covered by the systematic uncertainties.

In the third step the fitted numbers of events for the full signal region (2j1t) are used to calculate the numbers of events for the various processes surviving the cut on the NN output of 0.3 (0.4) in the muon (electron) channel. This extrapolation is done based on the NN output distributions of the different processes. Table 2 summarizes the fitted numbers of events for the different processes in the two channels after the cut on the NN discriminator. The cross section for *t* channel single top-quark production that corresponds to these numbers is consistent with predictions from theory [12] and recently published experimental results [4].

Figure 2 shows the distributions of the reconstructed top-quark transverse momentum and absolute value of the rapidity with the signal and background templates, normalized to the fit results. Electron and muon channel are combined by adding the p_{T} and $|y|$ distributions of the individual channels.

5 Differential cross section measurements

The aim of this analysis is to measure the cross section of single top-quark production as a function of kinematic variables of the process under study. However, the reconstructed distributions of the chosen variables (transverse momentum and absolute value of the rapidity of the top quark in Fig. 2) are distorted with respect to the parton-level distributions. The distortion is due to the fact that the event selection efficiency is not constant as a function of the kinematic variables and thus changes the spectra, and due to the resolution of the reconstruction of objects in the detector and ambiguities that are introduced in the course of reconstructing the events under the assumption of a signal event based on the objects measured in the detector. The latter effect leads to a migration of events with a parton-level value of the kinematic variable to a bin in the reconstructed distribution corresponding to a different value. The impact on the distributions from these two effects is illustrated in Fig. 3. In order to get the parton-level spectra, an unfolding method is applied to the reconstructed distributions, correcting for the mentioned detector and reconstruction effects. In this analysis the `TUnfold` algorithm [27], based on least-square fitting and Tikhonov regularization [28–30], is chosen.

Table 2: Event yield in the muon (electron) channel for a cut on the NN output distribution of $\mathit{Discriminator} > 0.3(0.4)$. The quoted uncertainties are the statistical uncertainties on the fit parameters.

Process	Events (muon channel)	Events (electron channel)
t channel	6618 $\pm$135	3307 $\pm$92
s channel	75 $\pm$31	43 $\pm$15
tW	508 $\pm$95	260 $\pm$53
$\mathrm{t\bar{t}}$	3638 $\pm$76	1985 $\pm$57
W+jets(heavy)	3366 $\pm$200	1360 $\pm$104
W+jets(light)	253 $\pm$90	129 $\pm$39
Z+jets	172 $\pm$51	57 $\pm$18
VV	58 $\pm$17	26 $\pm$9
Multijet QCD	1083 $\pm$55	375 $\pm$40
Total MC	15772 $\pm$297	7540 $\pm$170
Data	15843	7548

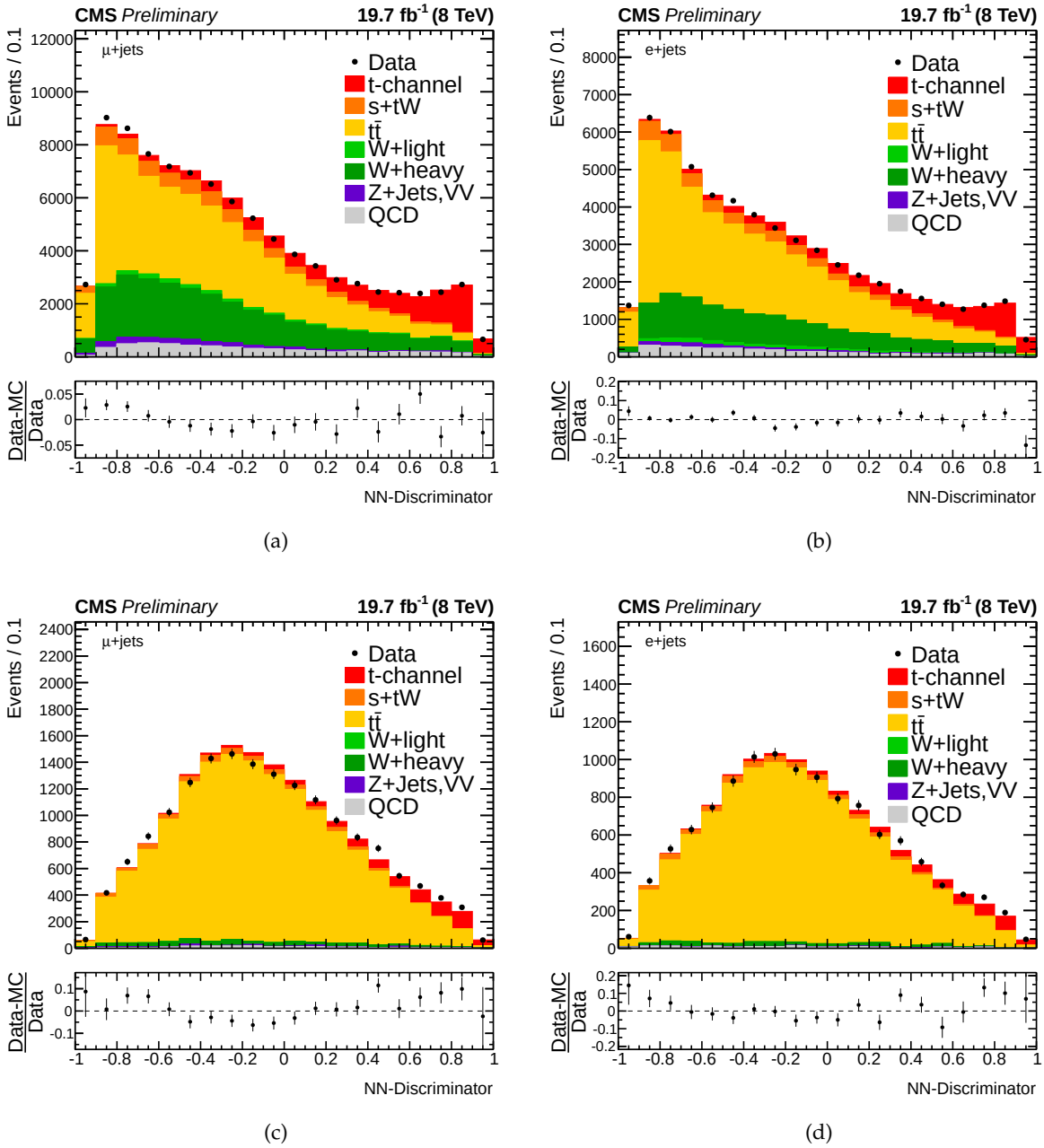

Figure 1: NN output distributions in the muon channel (left) and the electron channel (right). The upper row shows the 2j1t signal region, the lower row shows the 3j2t $t\bar{t}$ sideband region. The simulations of different processes are normalized to the fit results.

The background contributions are subtracted from the measured distributions using the templates from the background estimation, normalized to the fit results. The statistical uncertainties on the fit parameters and the correlations between them are taken into account and propagated to the final uncertainty of the unfolded distribution. The background-subtracted distributions are then further corrected by the unfolding procedure. A measured spectrum $\vec{w}$ can be written as the parton-level spectrum $\vec{x}$ multiplied with a smearing matrix S, $\vec{w} = S\vec{x}$. The smearing matrix S includes the two kinds of distortions, the non-uniform selection efficiency and the probability of events with a certain parton-level value of the kinematic variable

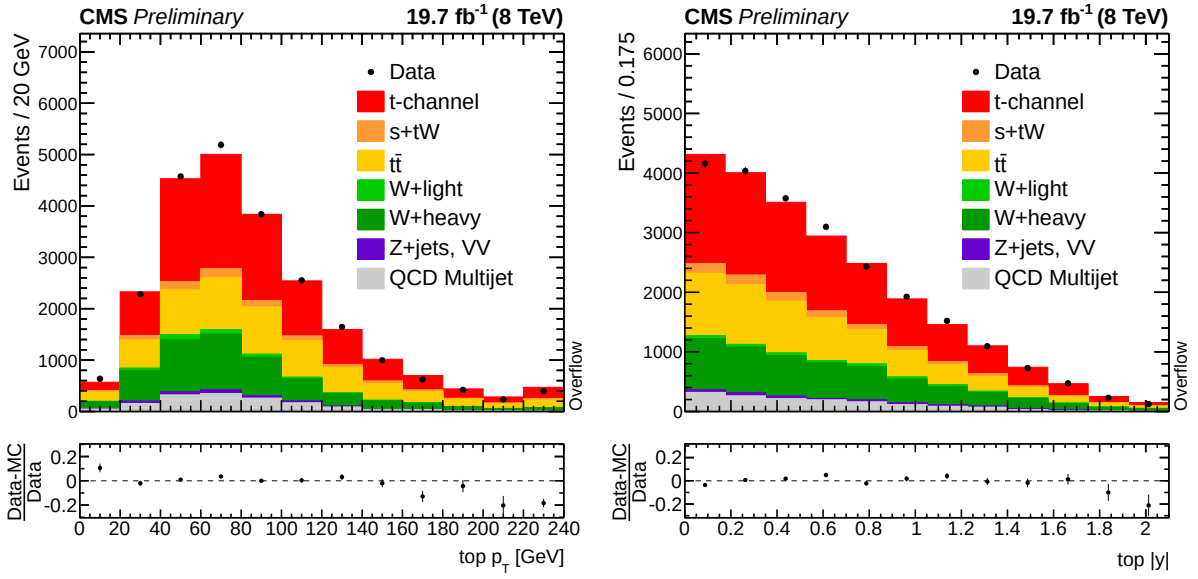

(a) (b)

Figure 2: Distributions of the reconstructed (a) top-quark p_{T} and (b) top-quark $|y|$ in the combined lepton+jets channel (electron and muon channel combined) with the cut on the NN discriminators applied. The simulations of the different processes are normalized to the fit results.

to be reconstructed in a different bin. The problem is solved by transforming $\vec{w} = S\vec{x}$ into a least-square problem. In order to stabilize the solution an additional regularization parameter is introduced. The optimal value for this regularization parameter is chosen based on the Minimum of Global Correlation method [30].

Twelve bins are used for the reconstructed spectrum and six bins are used for the unfolded distributions. The probability for an event with a reconstructed top-quark p_{T} ($|y|$) value in a certain range to have also a parton-level value of top-quark p_{T} ($|y|$) in the same range is called "purity" and can be estimated using simulated signal events. Similarly the "stability", which measures the probability of an event with a parton-level top-quark p_{T} ($|y|$) value in a certain range to have also a reconstructed value of top-quark p_{T} ($|y|$) in the same range, can be calculated. Both quantities have been checked for all six bins of the unfolded spectra and reasonable values between 50 and 80% have been obtained – only the stability of the sixth bin in top-quark $|y|$ is a bit lower with 32%.

While events with top-quark p_{T} (top-quark $|y|$) values beyond 240 GeV (2.1) are collapsed into the last visible bin in the reconstructed distributions shown in Fig. 2 (overflow bin), these events are not considered in the unfolding, i.e. only events with top-quark $p_{\mathrm{T}} < 240$ GeV (top-quark $|y| < 2.1$) are used to get the unfolded differential cross sections.

The results of the unfolding method are tested using pseudo experiments with simulated pseudo data sets. For each pseudo experiment the relative difference between the generated and unfolded distributions and the corresponding pull distributions are checked. The relative difference is the difference between unfolded and generated spectra divided by the generated spectrum in that bin. The pull for each of the bins is defined as the difference of unfolded and generated spectrum in that bin divided by the uncertainty on the unfolded spectrum in that

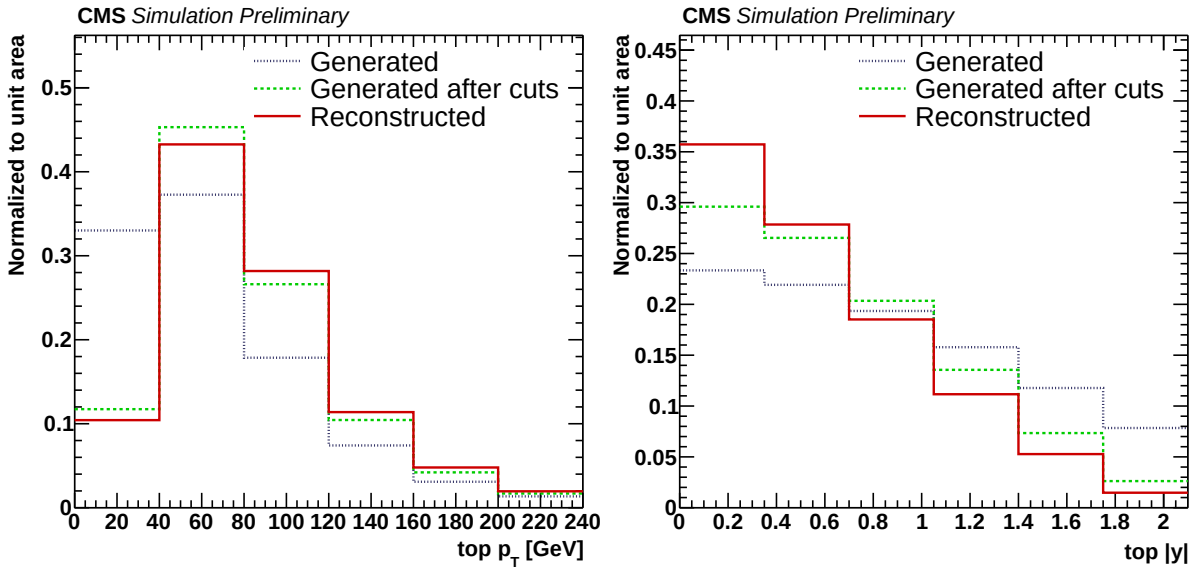

(a) (b)

Figure 3: Shape comparison of the transverse momentum (a) and the absolute value of the rapidity (b) of the single top quark on generator level without any selection, generated after selection cuts, and reconstructed after selection cuts in the combined lepton+jets channel.

bin. The results of these tests indicate that the unfolding is unbiased and the uncertainties are estimated correctly.

6 Systematic uncertainties

The resulting spectra of the top-quark p_{T} and top-quark $|y|$ are affected by various sources of systematic uncertainties, either due to detector resolution and reconstruction efficiencies or theoretical uncertainties in the modeling of signal and background processes. As the result is a normalized differential cross section, where the resulting spectrum is divided by the measured inclusive cross section, the effects of some of the systematic variations cancel out. The impact of the individual sources on the spectra is estimated by repeating the full chain of the analysis on the measured data. The default NN is applied to the signal and background samples that are affected by the systematic uncertainty under study and the resulting NN discriminator output distributions are used as fit templates for the background estimation. The top-quark p_{T} and $|y|$ templates from the varied background samples, normalized to the new background yields, are used for the background subtraction. The smearing matrix for the unfolding is determined from the varied signal MC templates, in case the source of systematic uncertainty under study affects also the signal process.

The sources of systematic uncertainty that have been studied are:

- Jet energy scale (JES): The impact from uncertainties in the jet energy scale is estimated by varying the jet energy corrections (JEC) within their p_{T}- and η-dependent uncertainties. The effect is propagated to the calculation of the missing transverse energy.
- Jet energy resolution (JER): Jet asymmetry measurements suggest that resolutions in

jet p_T are about 5% to 29% worse in data compared to simulation, depending on the jet's $|\eta|$ value. For that reason the distribution of reconstructed p_T for a fixed generated jet p_T is broader by the given percentage. The uncertainty on this measurement is about 6% to 20%, again depending on the jet $|\eta|$. To account for this difference, all jets in the simulated samples are scaled accordingly. The systematic uncertainty on this correction is estimated based on further smearings within the uncertainties of the used correction factors.

- Unclustered energy in $\vec{\not{E}}_T$: The energy contribution from all jets with $p_T < 10\,\text{GeV}$ and PF candidates not clustered into jets is called "unclustered energy". This energy contribution is varied by $\pm 10\%$ and the resulting uncertainty is propagated to the calculation of the missing transverse energy.
- b tagging: In order to estimate the uncertainty related to b tagging, the applied b-tagging scale factors are varied within their uncertainties. The variations are performed simultaneously for b- and c-quark jets, and they are combined in a common uncertainty. The scale factors for light-flavor jets are varied independently from the heavy-flavor scale factors and are treated as an independent mistag uncertainty.
- Pileup modelling: The events of all MC samples used in this analysis are reweighted such that the number of additional collision interactions (pileup) matches the number of pileup interactions in data. The latter is derived from the per-bunch-crossing instantaneous luminosity and the total proton-proton inelastic cross section. To account for uncertainties in the pileup distribution of data events, the reweighting parameters are varied within these uncertainties.
- Top-quark p_T reweighting in $t\bar{t}$ events: Differential cross section measurements [31] have shown that the p_T spectrum of the top quarks in $t\bar{t}$ events is significantly softer than the one generated by simulation programs. To correct for this effect the used events are reweighted according to scale factors derived from these measurements. As a measure of the resulting uncertainty, the measurement is performed with samples lacking any reweighting and with samples that have been reweighted twice.
- Top-quark mass: The impact of using a different top-quark mass from the nominal one in the generation of Monte Carlo events is estimated by using samples for t channel and $t\bar{t}$ events with top-quark masses differing by ± 1.5 GeV from the default value of 172.5 GeV.
- Electron and muon identification, isolation, and trigger: The uncertainties on the globally derived scale factors for electron and muon trigger, isolation, and ID are added in quadrature to the already applied scale factors.
- Q^2 scale: The uncertainties on the renormalization and factorization scales are studied with dedicated samples for $t\bar{t}$, W+jets and t channel single top-quark events. These samples are generated with twice and half the nominal Q value of the hard scattering process.
- Matching threshold: The impact of a higher and lower threshold for the matching of additional radiations from the matrix element and the parton shower is studied with dedicated samples for $t\bar{t}$ and W+jets.
- Muon resolution: The reconstruction of muons has been studied in Z decays. A transverse momentum resolution uncertainty of 0.6% is applied to all muons.
- QCD multijet modeling: The estimated rate of the QCD multijet template is scaled up by a factor of two to account for a potential mismodeling from the extraction in the anti-isolated region.

- Parton Distribution Functions (PDFs): The impact of different PDF sets (CT10, NNPDF2.1 and MSTW2008) and their uncertainty bands has been taken into account for the signal modeling according to the PDF4LHC recommendation [32].

The largest impact on the measurement stems from the variation of $\vec{\not{E}}_{\mathrm{T}}$, JES, and the renormalization and factorization scale of the $\mathrm{t\bar{t}}$ and W+heavy jets modeling.

7 Results

The unfolded distributions of the transverse momentum and the absolute value of the rapidity of the top quark in the combined lepton+jets channel are shown in Fig. 4, normalized to the measured inclusive cross section of the t channel single top-quark production, being the integral over all bins. The distributions from data are compared to the distributions generated with different MC generators: two NLO event generators, POWHEG and aMC@NLO, and COMPHEP [33, 34]. The main difference between the two NLO generators is the used flavor scheme. aMC@NLO uses the four-flavor scheme while POWHEG uses the five-flavor scheme, i.e. the b quarks in the initial state are included in the proton PDF. The COMPHEP sample consists of two separate samples, one with simulated $2 \to 2$ processes and one with simulated $2 \to 3$ processes, matched based on the p_{T} spectrum of the second b quark. For all three generators, the hadronization and parton shower is modelled by PYTHIA. All three simulations describe the unfolded data distribution well within the statistical and systematic uncertainties.

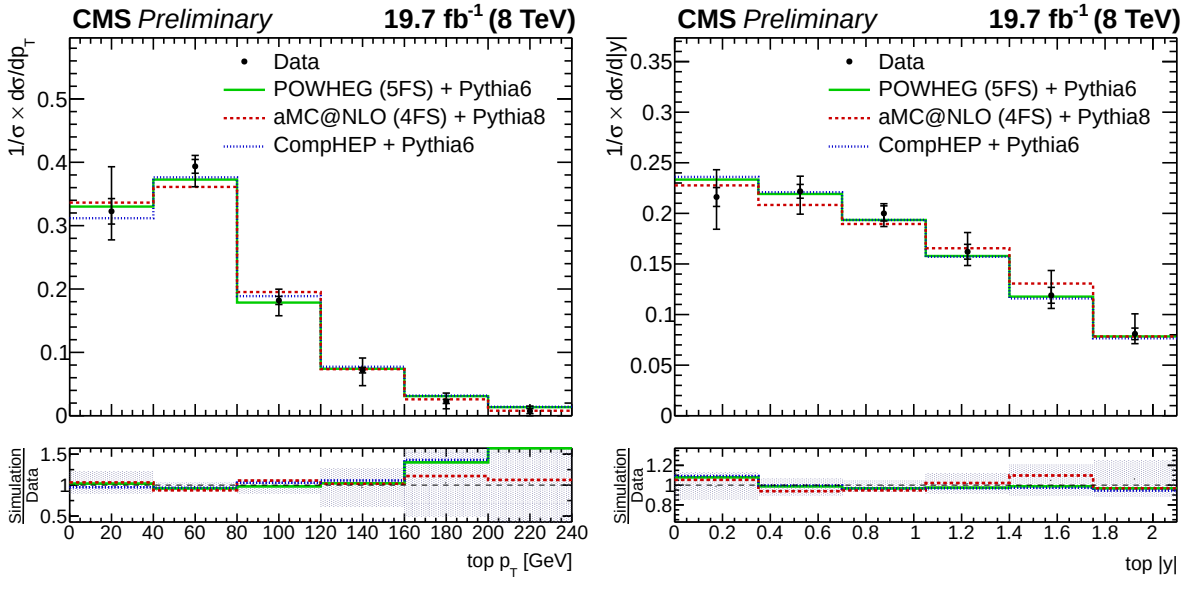

(a) (b)

Figure 4: Unfolded p_{T} spectrum (a) and unfolded $|y|$ spectrum (b) of the top quarks in the combined lepton+jets channel compared with the predictions from POWHEG+PYTHIA (solid), aMC@NLO+PYTHIA (dotted), and COMPHEP (dashed). The inner error bars indicate the statistical uncertainty while the outer error bars indicate the full (stat.+syst.) uncertainty.

8 Summary

The differential cross section of single top-quark production via the t channel has been measured as a function of the transverse momentum and as a function of the rapidity of the top quark using a dataset corresponding to a total integrated luminosity of 19.7 fb^{-1} at $\sqrt{s} = 8$ TeV, collected with the CMS detector. Overall, the unfolded data distributions are, within the estimated uncertainties, well described by the three MC predictions that have been compared in this analysis. As it is difficult to precisely model the top-quark kinematics for the single top-quark production in the t channel the agreement between the three different implementations as well as the agreement between the simulations and the data is impressive.

References

[1] CDF Collaboration, "First Observation of Electroweak Single Top Quark Production", *Phys.Rev.Lett.* **103** (2009) 092002, doi:10.1103/PhysRevLett.103.092002, arXiv:0903.0885.

[2] D0 Collaboration, "Observation of Single Top Quark Production", *Phys.Rev.Lett.* **103** (2009) 092001, doi:10.1103/PhysRevLett.103.092001, arXiv:0903.0850.

[3] ATLAS Collaboration, "Comprehensive measurements of t-channel single top-quark production cross sections at $\sqrt{s} = 7$ TeV with the ATLAS detector", arXiv:1406.7844.

[4] CMS Collaboration, "Measurement of the t-channel single-top-quark production cross section and of the $| V_{tb} |$ CKM matrix element in pp collisions at $\sqrt{s}$= 8 TeV", *JHEP* **1406** (2014) 090, doi:10.1007/JHEP06(2014)090, arXiv:1403.7366.

[5] J. M. Campbell, R. Frederix, F. Maltoni, and F. Tramontano, "Next-to-Leading-Order Predictions for t-Channel Single-Top Production at Hadron Colliders", *Phys.Rev.Lett.* **102** (2009) 182003, doi:10.1103/PhysRevLett.102.182003, arXiv:0903.0005.

[6] S. Frixione, P. Nason, and C. Oleari, "Matching NLO QCD computations with Parton Shower simulations: the POWHEG method", *JHEP* **0711** (2007) 070, doi:10.1088/1126-6708/2007/11/070, arXiv:0709.2092.

[7] S. Alioli, P. Nason, C. Oleari, and E. Re, "A general framework for implementing NLO calculations in shower Monte Carlo programs: the POWHEG BOX", *JHEP* **1006** (2010) 043, doi:10.1007/JHEP06(2010)043, arXiv:1002.2581.

[8] S. Alioli, P. Nason, C. Oleari, and E. Re, "NLO single-top production matched with shower in POWHEG: s- and t-channel contributions", *JHEP* **0909** (2009) 111, doi:10.1088/1126-6708/2009/09/111,10.1007/JHEP02(2010)011, arXiv:0907.4076.

[9] E. Re, "Single-top Wt-channel production matched with parton showers using the POWHEG method", *Eur. Phys. J. C* **71** (2011) 1547, doi:10.1140/epjc/s10052-011-1547-z, arXiv:1009.2450.

[10] T. Sjöstrand, S. Mrenna, and P. Z. Skands, "PYTHIA 6.4 Physics and Manual", *JHEP* **0605** (2006) 026, doi:10.1088/1126-6708/2006/05/026, arXiv:hep-ph/0603175.

[11] J. Alwall et al., "MadGraph 5 : Going Beyond", *JHEP* **1106** (2011) 128, doi:10.1007/JHEP06(2011)128, arXiv:1106.0522.

[12] N. Kidonakis, "Differential and total cross sections for top pair and single top production", doi:10.3204/DESY-PROC-2012-02/251, arXiv:1205.3453.

[13] M. Czakon and A. Mitov, "Top++: A Program for the Calculation of the Top-Pair Cross-Section at Hadron Colliders", *Comput.Phys.Commun.* **185** (2014) 2930, doi:10.1016/j.cpc.2014.06.021, arXiv:1112.5675.

[14] K. Melnikov and F. Petriello, "Electroweak gauge boson production at hadron colliders through $\mathcal{O}(\alpha_S^2)$", *Phys. Rev. D* **74** (2006) 114017, doi:10.1103/PhysRevD.74.114017, arXiv:hep-ph/0609070.

[15] J. M. Campbell and R. K. Ellis, "Radiative corrections to Z b anti-b production", *Phys.Rev.* **D62** (2000) 114012, doi:10.1103/PhysRevD.62.114012, arXiv:hep-ph/0006304.

[16] CMS Collaboration, "Particle-Flow Event Reconstruction in CMS and Performance for Jets, Taus, and $\not\!\!E_{\mathrm{T}}$", CMS Physics Analysis Summary PFT-09-001, 2009.

[17] CMS Collaboration, "Commissioning of the particle flow event reconstruction with the first LHC collisions recorded in the CMS detector", CMS Physics Analysis Summary PFT-10-001, 2010.

[18] CMS Collaboration, "Performance of CMS muon reconstruction in pp collision events at $\sqrt{s} = 7$ TeV", *JINST* **7** (2012) P10002, doi:10.1088/1748-0221/7/10/P10002, arXiv:1206.4071.

[19] CMS Collaboration, "Electron reconstruction and identification at sqrt(s) = 7 TeV", *CMS-PAS-EGM-10-004* (2010).

[20] S. D. Ellis and D. E. Soper, "Successive combination jet algorithm for hadron collisions", *Phys.Rev.* **D48** (1993) 3160–3166, doi:10.1103/PhysRevD.48.3160, arXiv:hep-ph/9305266.

[21] M. Cacciari, G. P. Salam, and G. Soyez, "The anti-k_t jet clustering algorithm", *JHEP* **04** (2008) 063, doi:10.1088/1126-6708/2008/04/063, arXiv:0802.1189.

[22] CMS Collaboration, "Jet Performance in pp Collisions at $\sqrt{s}$=7 TeV", CMS Physics Analysis Summary CMS-PAS-JME-10-003, 2010.

[23] CMS Collaboration, "Identification of b-quark jets with the CMS experiment", *JINST* **8** (2013) 04013, doi:10.1088/1748-0221/8/04/P04013, arXiv:1211.4462.

[24] M. Feindt, "A Neural Bayesian Estimator for Conditional Probability Densities", *arXiv:physics/0402093* (2004) arXiv:physics/0402093.

[25] M. Feindt and U. Kerzel, "The NeuroBayes neural network package", *Nucl. Instrum. Meth.* **A559** (2006) 190–194, doi:10.1016/j.nima.2005.11.166.

[26] T. Chwalek, "Measurement of the W-Boson Helicity-Fractions in Top-Quark Decays with the CDF II Experiment and Prospects for an Early $t\bar{t}$ Cross-Section Measurement with the CMS Experiment", *PhD Thesis, Karlsruhe Institute of Technology,* **IEKP-KA/2010-5, CERN-THESIS-2010-255** (2010).

[27] S. Schmitt, "TUnfold, an algorithm for correcting migration effects in high energy physics", *Journal of Instrumentation* **7** (2012), no. 10, T10003.

[28] A. Tikhonov, "Solution of incorrectly formulated problems and the regularization method", *Soviet Mathematics Doklady* **4** (1963) 1035–1038.

[29] V. Blobel, "An Unfolding method for high-energy physics experiments", arXiv:hep-ex/0208022.

[30] V.Blobel, "Unfolding - Linear Inverse Problems", *Notes for the Terascale Workshop on Unfolding and Data Correction at DESY* (2010).

[31] CMS Collaboration, "Measurement of differential top-quark pair production cross sections in the lepton+jets channel in pp collisions at 8 TeV", *CMS Physics Analysis Summary* **TOP-12-027** (2013).

[32] M. Botje et al., "The PDF4LHC Working Group Interim Recommendations", arXiv:1101.0538.

[33] CompHEP Collaboration, "CompHEP 4.4: Automatic computations from Lagrangians to events", *Nucl.Instrum.Meth.* **A534** (2004) 250–259, doi:10.1016/j.nima.2004.07.096, arXiv:hep-ph/0403113.

[34] A. Pukhov et al., "CompHEP: A Package for evaluation of Feynman diagrams and integration over multiparticle phase space", arXiv:hep-ph/9908288.